

Time-Resolved IR Spectroscopy

Direct Observation of a Hydrogen-Bonded Charge-Transfer State of 4-Dimethylaminobenzonitrile in Methanol by Time-Resolved IR Spectroscopy**

Wai-Ming Kwok, Michael W. George, David C. Grills, Chensheng Ma,* Pavel Matousek, Anthony W. Parker, David Phillips, William T. Toner, and Michael Towrie

Charge-transfer excited states have frequently been studied by using 4-dimethylaminobenzonitrile (DMABN) as a model. In nonpolar solvents, a single fluorescence band is observed from a locally excited (LE) state. In polar solvents, the initially populated LE state reacts further to produce a stable intramolecular charge-transfer (ICT) state, which gives rise to

a second fluorescence band that overlaps with, but is abnormally red-shifted from, the LE emission.^[1] Results of experiments using aprotic solvents are well described by models in which polarity is the only solvent property that affects the charge transfer reaction activation energy and the relative stabilization of the ICT and LE states.^[2] Whilst much work continues to concentrate on determining the structures of the LE and ICT states,^[3–7] the precise nature of the difference between the properties of the excited state in protic and aprotic solvents is little understood. For example, the fluorescence quantum yield of DMABN in protic solvents is lower and the fluorescence spectrum is further red-shifted and broadened, relative to measurements in aprotic solvents of the same polarity,^[8,9] and the fluorescence decay kinetics are difficult to interpret.^[2] Hydrogen bonding in protic solvents can lead to complicated interactions^[10] but although specific solute–solvent and solute–solute interactions have been discussed,^[8,11–14] there is no generally accepted explanation. There are similar problems in other cases of dual fluorescence.^[15]

The time-resolved infrared (TRIR) absorption spectra presented here demonstrate and monitor the formation of a hydrogen-bonded charge-transfer state of photoexcited DMABN in the protic solvent methanol (MeOH), through the development of the $\text{C}\equiv\text{N}$ IR absorption band from an initial singlet into a doublet. The initial single band is interpreted as belonging to an ICT state like that created in aprotic acetonitrile (MeCN), where only one absorption band is observed at all delay times. The second component is interpreted as being due to the hydrogen-bonded charge-transfer state; the kinetics show the populations of the free and hydrogen-bonded species coming to dynamic equilibrium. We designate the hydrogen-bonded state as HICT. This is the first direct observation of hydrogen bonding in an excited state. Since the populations in the LE state and the two charge-transfer states coexist, the fluorescence will be triple, not dual in character. Neglect of this major factor is considered to account for much of the difficulty in interpreting the fluorescence results.^[2,8,11–13] A mechanism of this kind has not to our knowledge been proposed before. We believe this interpretation is applicable to other molecules with solvent-dependent dual fluorescence.

Figure 1 shows TRIR spectra of DMABN in MeCN (a) and MeOH (b) recorded with sub-picosecond time resolution at pump–probe delays from 2 to 3000 ps after excitation; Figure 2 gives the time-dependence of the absorption band areas. Kinetics parameters were determined by least-squares fits. The spectral region between 2065 and 2235 cm^{-1} (Figure 1) covers the $\text{C}\equiv\text{N}$ bands of the ground, LE, and ICT states.^[3,4,6,16] The LE band is observed by Raman but not by TRIR spectroscopy.^[6,16]

The ICT state $\text{C}\equiv\text{N}$ IR absorption band at 2104 cm^{-1} in MeCN and the ground state depletion (bleach) at 2213 cm^{-1} are clearly seen (Figure 1a). Time constants for the non-radiative reaction $\text{LE} \rightleftharpoons \text{ICT}$ plus the decay of the whole population (lines in Figure 2a) are 6.4 ps (equilibration) and 2.7 ns (decay). The small level of decay back to the ground state is shown by the small recovery in the bleached signal and is due to fluorescence and internal conversion (IC) to the

[*] Dr. C. Ma,⁺ Dr. W.-M. Kwok,⁺ Prof. D. Phillips
Department of Chemistry
Imperial College
Exhibition Road, London SW7 2AY (UK)
Fax: (+44) 207-594-5801
E-mail: macs@hkucc.hku.hk

Dr. M. W. George, Dr. D. C. Grills
School of Chemistry
University of Nottingham
University Park, Nottingham NG7 2RD (UK)

Dr. P. Matousek, Dr. A. W. Parker, Dr. M. Towrie
Central Laser Facility
CLRC Rutherford Appleton Laboratory
Didcot, Oxfordshire OX11 0QX (UK)

W. T. Toner
Department of Physics
Clarendon Laboratory
Parks Road, Oxford OX1 3PU (UK)

[**] We are grateful to the EPSRC for financial support through grants GR/R29062 and GR/M40486. This work was carried out at the Central Laser Facility, CLRC Rutherford Appleton Laboratory.

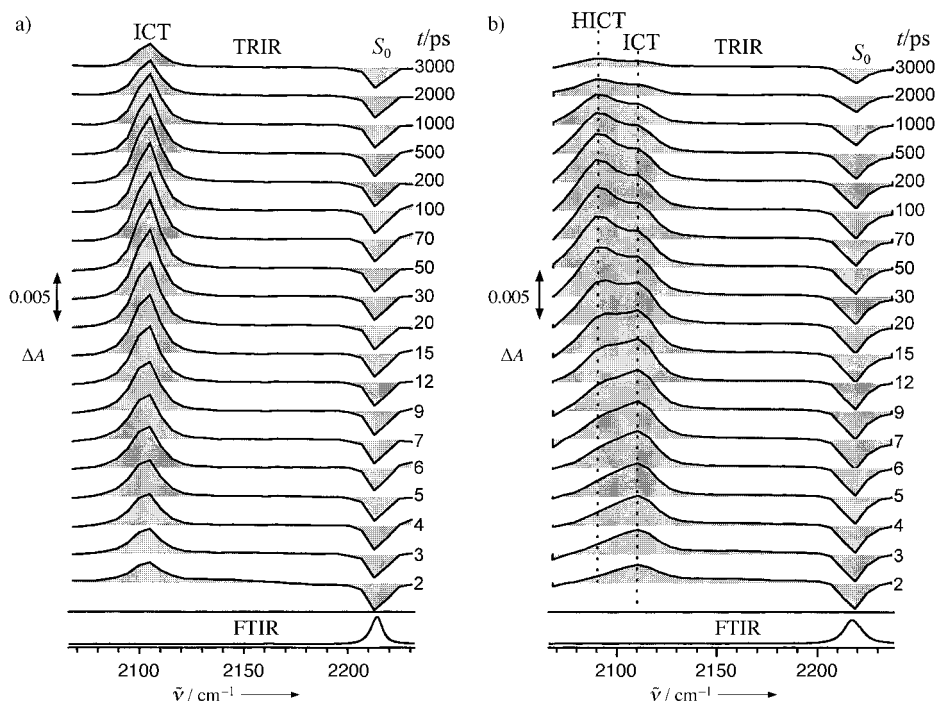


Figure 1. Ground-state FTIR and TRIR spectra of DMABN in MeCN (a) and in MeOH (b), which were obtained at different pump–probe time delays with excitation at 267 nm.

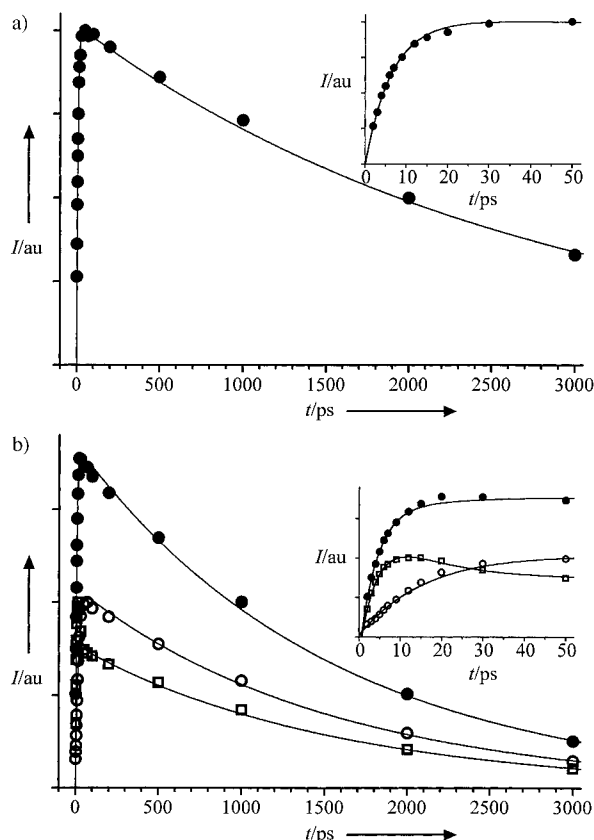


Figure 2. a) Time-dependence of the ICT state C≡N band areas in Figure 1a (●). b) Time-dependence of the charge-transfer C≡N band areas in Figure 1b: total (●); ICT, band centered at 2109 cm^{-1} , (□); HICT, band centered at 2091 cm^{-1} , (○). Solid lines are results of fits (see text). The inserts give details of the early time kinetics.

ground state, the lack of triplet decay providing a constant remainder on the 3 ns time scale. From fits to the bleached band areas from 20 ps to 3 ns (not shown) using the absorption decay time constant, and from the fluorescence quantum yield (0.030),^[9] we estimate the rates for fluorescence ($1.1 \times 10^7 \text{ s}^{-1}$), IC ($\approx 6 \times 10^7 \text{ s}^{-1}$), and intersystem crossing (ISC) to the triplet ($\approx 30 \times 10^7 \text{ s}^{-1}$). We have observed similar TRIR spectra in THF and triacetin (1,2,3-propanetriol triacetate), but with different time constants. The equilibrium LE/ICT population ratio in MeCN may be estimated to be about 1 % from steady-state fluorescence spectra. Our results agree with those of many fluorescence studies:^[2] prompt formation of the LE state is followed by fast equilibration of the LE and ICT populations, the parameters for which vary mainly with polarity in aprotic solvents of low viscosity.

The results obtained are very different in MeOH (Figure 1b and 2b). As the C≡N absorption grows, the band can be resolved into two components at 2091 and 2109 cm^{-1} , which reach constant relative intensities by about 50 ps. These data were fitted by using Lorentzians of equal width to separate the components, but essentially the same results were also obtained by using the total intensity and mean frequency of the combined bands plus the estimated separation of the peaks at late time. Thus, we believe it is unnecessary in this brief account to consider possible small non-Lorentzian effects.^[17] Moreover, the main qualitative conclusions of this time-resolved experiment are clear from a comparison of Figure 1a and b.

The total intensity of the two components in MeOH has time constants of 5.5 ps and 1.6 ns for growth and decay, respectively, and the component at 2091 cm^{-1} grows with a time constant of 13 ps (lines in Figure 2b) but is not

resolvable at the earliest times. The bandwidths of the two components are significantly broader than the ground state bleach (at 2217 cm^{-1}), indicating that some unidentified faster processes or inhomogeneous effects are also involved. Ground state bleach recovery can be seen in Figure 1b, and the enhancement relative to the behavior in MeCN indicates much stronger internal conversion in MeOH. By using the fluorescence quantum yield of DMABN in MeOH (0.017)^[9] in fits to the bleach areas from 20 ps to 3 ns as before (not shown), the fluorescence, IC, and ISC rates are found to be 1.1×10^7 , $\approx 31 \times 10^7$, and $\approx 30 \times 10^7\text{ s}^{-1}$, respectively. The LE equilibrium population fraction is again estimated to be very small and these rates are taken to apply to the charge-transfer state(s). Qualitatively similar results were obtained in ethanol and butanol. Asymmetry of the DMABN $\text{C}\equiv\text{N}$ band in protic solvents consistent with this work is visible—though not commented on—in published TR³^[3] and TRIR⁴^[4] spectra.

The growth of the component at 2091 cm^{-1} at the expense of that at 2109 cm^{-1} is clearly due to an interaction that occurs in protic MeOH after charge separation and does not occur in aprotic MeCN. We attribute it to hydrogen bonding between the MeOH and the ICT state of DMABN. The shift to lower wavenumber by 108 cm^{-1} of the initial component (at 2109 cm^{-1}) from the ground state bleach (at 2217 cm^{-1}) differs by only 1 cm^{-1} from that observed for the ICT in MeCN, so we attribute it to a state closely resembling the “free” ICT state formed in aprotic solvents, and assign the second component at 2091 cm^{-1} to the hydrogen-bonded form. We designate these two charge-transfer states as ICT and HICT, respectively. The 13 ps time scale for the growth of the 2091 cm^{-1} (HICT) band is consistent with the 10–15 ps time scale observed for the hydrogen bonding of ground state *N*-methylacetamide in MeOH.^[18] The 20 cm^{-1} separation of the $\text{C}=\text{O}$ components in that case is comparable with the 18 cm^{-1} $\text{C}\equiv\text{N}$ splitting we observe, and the resolution of the components is similar. The strongly enhanced rate for IC to the ground state is consistent with the large effect of deuteration on DMABN fluorescence in alcohol solvents,^[11] and we note that deactivation via IC resulting from hydrogen bonding has been proposed to account for the fluorescence quenching of many molecules having ICT states.^[19]

Our results show that the rates for radiative decay and ISC are unaffected by hydrogen bonding, illustrating the weakness of this interaction. It therefore seems reasonable to assume the “free” ICT in MeOH is the same as that in MeCN, in which case it follows that the radiative rates will be the same for ICT and HICT. Taking the ICT state also to have the same nonradiative decay rates in MeOH and MeCN leads to the conclusion that the enhanced IC rate in MeOH is wholly attributable to the HICT state (or nearly so). The IC rate for this fraction of the charge-transfer population (see below) is thus estimated to be about 50 % larger than the value quoted above for the mixture.

The kinetics are well described (lines in Figure 2b) by a sequence of reversible, nonradiative reactions that lead to equilibrium populations on picosecond time scales: $S_0 \xrightarrow{h\nu} \text{LE} \rightleftharpoons \text{ICT} \rightleftharpoons \text{HICT}$, with each excited state also decaying on the nanosecond time scale as discussed earlier. The small population of the HICT state relative to the ICT state at $t=0$

indicated by our fits (less than $\approx 15\%$ of the total) justifies neglect of a further possible reaction, $\text{LE} \rightleftharpoons \text{HICT}$, but does not exclude it. The results are insensitive to the method used to separate the two components, as noted above, but their detailed interpretation using the kinetics model depends on the ratio of ICT to HICT IR absorption cross sections, which are not known. For example, if we vary the assumed ratio from 0.75 to 1.6, the equilibration time constant for $\text{LE} \rightleftharpoons \text{ICT}$ rises from ~ 4 to 8 ps, while that for $\text{ICT} \rightleftharpoons \text{HICT}$ falls from ~ 12 to 8 ps and the forward $\text{ICT} \rightarrow \text{HICT}$ reaction time constant falls from ~ 20 to 11 ps. The estimated equilibrium HICT population fraction rises from 56 % to 73 % over the same parameter range. These ranges are not large and since the LE equilibration time constant in MeOH is expected to be similar to that in MeCN (6.4 ps) because of the similar polarity of the two solvents, we conclude that the most probable $\text{C}\equiv\text{N}$ IR absorption cross section ratio of ICT and HICT is close to unity. The assumption of equal cross sections is also made and justified in reference [17]. The population fraction in HICT at equilibrium is thus close to two thirds and the $\text{ICT} \rightleftharpoons \text{HICT}$ equilibration time constant is ≈ 10 ps. This is very similar to the results obtained by Woutersen et al.^[18]

We consider these results to be compelling evidence for the coexistence of two charge-transfer states of photoexcited DMABN in MeOH, one similar to the “free” ICT state formed in MeCN, and the other hydrogen-bonded.

Intermolecular solute–solvent hydrogen bonding interactions are highly sensitive to solute–solvent orientation and distance, and the formation process must also compete with the tendency of MeOH to form solvent–solvent multimers. It is therefore significant that the estimated time constant for the forward hydrogen-bonding reaction is close to the 15.8 ps time scale^[20] for solvent–solvent bond breaking and R–OH rotation in MeOH. The strength of the intermolecular forces will clearly be critical. FTIR spectra of the DMABN ground state show the $\text{C}\equiv\text{N}$ stretch occurs at 2217 cm^{-1} in MeOH and at 2213 cm^{-1} in MeCN, the band being somewhat broader in MeOH (Figure 1). The shift to higher wavenumbers in MeOH is close to the 5 cm^{-1} upshift observed for the “free” ICT state in the TRIR spectrum recorded in MeOH relative to that in MeCN (Figure 1). Since we observe that the frequency of the hydrogen-bonded component in the excited state is lowered, we attribute the ground state upshift and broadening to a weaker interaction that does not produce stable bonding. The LE state is not observed in this experiment but it is clear from Figure 1b that the hydrogen-bonded component at 2091 cm^{-1} has little or no intensity at the earliest times, and grows at the expense of the free component, so whatever bonding interaction there may be with the LE state is again weak. The charge-separation step is thus seen to be necessary to favor DMABN–MeOH configurations that form bonds having lifetimes of a few picoseconds so that the majority of the DMABN excited state population becomes hydrogen-bonded, despite the strong MeOH–MeOH interaction. We consider that the increased negative charge density on the cyano electron-acceptor region of the ICT state of DMABN^[3,4] facilitates bonding at this site in the presence of a proton donor, such as the -OH group in alcohol, the electron acceptor group in turn becoming a proton acceptor.

Our TRIR results can be briefly discussed in relation to the fluorescence properties of the ICT state of DMABN. As noted above, we consider that the radiative rate is most likely the same for ICT and HICT. The charge-transfer fluorescence will therefore be composed of overlapping bands having intensities in proportion to the ICT/HICT population ratio of about 1/2. The overall fluorescence will be intrinsically triple, and show complicated kinetics^[21,22] not predicted by the dual fluorescence model^[2] appropriate for aprotic solvents. This can account for much of the confusion in the literature, especially the complicated fluorescence decay dynamics observed at different temperatures in alcohols,^[2,22] where variations in the relative populations of LE/ICT and ICT/HICT can be expected. Interpretations using more subtle effects of dielectric relaxation and viscosity (undoubtedly also relevant) will clearly not succeed when such a major factor is neglected.

The steady-state fluorescence spectrum has no visible structure to help separate the two charge-transfer components although the spectrum in MeOH is broader than in MeCN, and the red shift of the maximum by about 1000 cm⁻¹ in MeOH appears to be largely due to the increase of about 2000 cm⁻¹ in the width (FWHM),^[9] rather than a large shift of electronic origin of the kind separating LE from ICT. It may be possible to resolve these two components experimentally by measuring the transient resonance Raman excitation profiles (REPs) of the ICT and HICT states, thus providing new opportunities for studying the differences between them.

Only the C≡N region was covered in this experiment, but since the phenyl ring is also part of the electron-acceptor group,^[3,4] other bands may also be affected, as well as the structural configuration. We note that two hydrogen-bonding sites have been reported for ground state 4-aminobenzonitrile in water.^[23] Further work on DMABN and its analogues is in progress and includes studying the structural differences between ICT and HICT and the complex interplay of temperature-dependent molecular and solvent properties that can affect the excited state spectra.

In conclusion, our data demonstrate the existence of two charge-transfer states of photoexcited DMABN in MeOH, namely ICT and HICT, where HICT is hydrogen-bonded. ICT is populated from the LE state and a dynamic equilibrium between the populations of the two charge-transfer states is established on a 13 ps time scale. The internal conversion de-excitation rate of the HICT state is much larger than that of ICT and is mainly responsible for the reduced quantum yield in MeOH. The overall fluorescence spectrum is composed of contributions from LE, ICT, and HICT. We have proposed that this novel three-state mechanism can account for many anomalies in the fluorescence spectra of dual fluorescence molecules in protic solvents. The results also illustrate the power of the high-resolution, high-sensitivity TRIR technique employed and the ability to monitor the formation of bonds between excited states in real time.

Experimental Section

Measurements were made using the Picosecond Infrared Absorption and Transient Excitation (PIRATE) system.^[24] Samples at room

temperature (23°C) were excited at a 1 kHz repetition rate by a 267 nm pump beam (0.2 ps, 5 μJ per pulse; 200 μm diameter), produced by frequency-tripling a fraction of the 800 nm regenerative amplifier output. A solution (5 mM) of triple-recrystallized DMABN in spectroscopic grade solvent was circulated to ensure fresh material was exposed on every shot. The femtosecond signal and idler outputs of an optical parametric amplifier (OPA), pumped by the remaining 800 nm beam, were mixed in silver gallium sulfide (AgGaS₂) to give a broadband IR beam. Absorption spectra were obtained as described elsewhere.^[24] Briefly, the sub-picosecond IR beam is split into probe and reference beams using a 50% germanium beam splitter. The probe beam is focused to about 150 μm diameter in the sample cell, and the transmitted light is imaged onto a spectrometer. The reference arm has similar optics. Transmitted and reference spectra are recorded on 64-element MIR array detectors with 5 cm⁻¹ resolution, read out on each shot, and normalized point-by-point. This gives good comparability and sensitivity for all bands in a 200 cm⁻¹ range selected by tuning the OPA.

Received: July 25, 2002

Revised: December 5, 2002 [Z19816]

Keywords: charge transfer · cyanides · fluorescence · hydrogen bonds · IR spectroscopy · time-resolved spectroscopy

- [1] E. Lippert, W. Rettig, V. Bonacic-Koutecky, F. Heisel, J. A. Míche, *Adv. Chem. Phys.* **1987**, 68, 1–173.
- [2] P. Changenet, P. Plaza, M. M. Martin, Y. H. Meyer, *J. Phys. Chem. A* **1997**, 101, 8186–8194, and references therein.
- [3] W. M. Kwok, C. Ma, P. Matousek, A. W. Parker, D. Phillips, W. T. Toner, M. Towrie, S. Umaphathy, *J. Phys. Chem. A* **2001**, 105, 984–990.
- [4] M. Hashimoto, H. Hamaguchi, *J. Phys. Chem.* **1995**, 99, 7875–7877.
- [5] H. Okamoto, H. Inishi, Y. Nakamura, S. Kohtani, R. Nakagaki, *J. Phys. Chem. A* **2001**, 105, 4182–4188.
- [6] C. Chudoba, A. Kummrow, J. Dreyer, J. Stenger, E. T. J. Nibbering, T. Elsaesser, K. A. Zachariasse, *Chem. Phys. Lett.* **1999**, 309, 357–363.
- [7] J. Dobkowski, J. Wojcik, W. Kozminski, R. Kolos, J. Waluk, J. Michl, *J. Am. Chem. Soc.* **2002**, 124, 2406–2407.
- [8] D. Pilloud, P. Suppan, L. V. Haelst, *Chem. Phys. Lett.* **1987**, 137, 130–133.
- [9] T. Okada, M. Uesugi, G. Kohler, K. Rechthaler, K. Rotkiewicz, W. Rettig, G. Grabner, *Chem. Phys.* **1999**, 241, 327–337.
- [10] a) C. Chudoba, E. T. J. Nibbering, T. Elsaesser, *Phys. Rev. Lett.* **1998**, 81, 3010–3013; b) C. Chudoba, E. T. J. Nibbering, T. Elsaesser, *J. Phys. Chem. A* **1999**, 103, 5625–5628.
- [11] R. J. Visser, C. A. G. O. Varma, J. Konijnenberg, P. Bergwerf, *J. Chem. Soc. Faraday Trans. 2* **1983**, 79, 347–367.
- [12] C. Cazeau-Dubroca, S. A. Lyazidi, P. Cambou, A. Peirigua, P. Cazeau, M. Pesquer, *J. Phys. Chem.* **1989**, 93, 2347–2358.
- [13] O. S. Khalil, R. H. Hofeldt, S. P. McGlynn, *J. Lumin.* **1973**, 6, 229–244.
- [14] K. A. Zachariasse, T. Yoshihara, S. I. Druzhinin, *J. Phys. Chem. A* **2002**, 106, 6325–6333.
- [15] P. R. Bangal, S. Panja, S. Chakravorti, *J. Photochem. Photobiol. A* **2001**, 139, 5–16.
- [16] C. Ma, W. M. Kwok, P. Matousek, A. W. Parker, D. Phillips, W. T. Toner, M. Towrie, *J. Phys. Chem. A* **2002**, 106, 3294–3305.
- [17] M. Besnard, M. I. Cabaco, F. Strehle, J. Yarwood, *Chem. Phys.* **1992**, 163, 103–114.
- [18] S. Woutersen, Y. Mu, G. Stock, P. Hamm, *Chem. Phys.* **2001**, 266, 137–147.

- [19] A. Morimoto, T. Yatsushashi, T. Shimada, S. Kumazaki, K. Yoshihara, H. Inoue, *J. Phys. Chem. A* **2001**, 105, 8840–8849, and references therein.
- [20] M. L. Horng, J. A. Gardecki, A. Papazyan, M. Maroncelli, *J. Phys. Chem.* **1995**, 99, 17311–17337.
- [21] S. R. Meech, D. Phillips, *J. Chem. Soc. Faraday Trans. 2* **1987**, 83, 1941–1956.
- [22] S.-G. Su, J. D. Simon, *J. Chem. Phys.* **1988**, 89, 908–919.
- [23] E. Alejandro, J. A. Fernandez, F. Castano, *Chem. Phys. Lett.* **2002**, 353, 195–203.
- [24] M. Towrie, D. C. Grills, J. Dyer, J. A. Weinstein, P. Matousek, R. Barton, P. D. Bailey, N. Subramaniam, W. M. Kwok, C. Ma, D. Phillips, A. W. Parker, M. W. George, *Appl. Spectrosc.* **2003**, 57, 367–380.